Coke Formation over a Nickel Catalyst under Methane Dry Reforming Conditions: Thermodynamic and Kinetic Models

Jason M. Ginsburg,[†] Juliana Piña,[‡] Tarek El Solh,[§] and Hugo I. de Lasa*,[†]

Chemical Reactor Engineering Centre, Faculty of Engineering, University of Western Ontario, London, Ontario, Canada N6A 5B9, Department of Chemical Engineering, PLAPIQUI, Universidad Nacional del Sur, CONICET, Camino La Carrindaga km. 7, (8000) Bahía Blanca, Argentina, and Imperial Oil Research Center, Sarnia, Ontario, Canada N7T 8C8

The CO_2 reforming of methane is studied over a 20 wt % Ni/USY-zeolite, and more specifically, a thermodynamic analysis of the formation of coke is used as a basis for the kinetic modeling of coke phenomena that exist under dry reforming conditions. Two thermodynamic parameters, α and β, are compared to the equilibrium constants for the CH_4 decomposition and the CO disproportionation reactions and defined to determine whether coke formation is favored. This thermodynamic analysis elucidates the significance of the CO disproportionation reaction on the amount of coke deposited over the catalyst under consideration. A kinetic model with negative overall order of one, with respect to the partial pressure of carbon monoxide, is found as the most accurate prediction of the rate of coke formation. This type of kinetics strongly suggests the requirement of three adjacent free catalyst sites for the coking reaction to proceed under allowable thermodynamic conditions.

Introduction

Dry reforming of methane over various metal catalysts has received much attention in recent years.[1,2] This renewed interest stems from the fact that both CO_2 and CH_4 are major greenhouse gases; thus, the utilization of these reactants in many chemical processes could drastically improve the quality of the environment.[3,4] Important advantages that this reaction offers over steam reforming are (a) the formation of a suitable H_2/CO ratio for use in Fischer−Tropsch synthesis and (b) more desirable thermodynamic properties (i.e., large heat of reaction and reversibility) for chemical energy transmission systems (CETS).[1,5] Although the dry reforming concept has environmental benefits and economic advantages, there are only a few commercial processes based on the CO_2 reforming reaction (i.e., the CALCOR[6] and SPARG[7] processes). The success of the concept is highly dependent on the catalyst activity and selectivity. From an industrial point of view, it is more practical to develop and optimize Ni-based catalysts, as these are the most viable given the high cost of noble metals.[2] A major limitation that arises from the use of nickel is the formation of carbon deposits, which can cause significant deactivation of the catalyst.

One promising approach for the dry reforming concept is the Catforming process, proposed at CREC-UWO, which consists of two circulating fluid beds: i.e., a downer for the endothermic CO_2 reforming and a riser for the catalyst regeneration. The transport of the solids between both reactors allows for a period of catalyst regeneration involving coke combustion.[8] Despite the fact that the Catformer is to be operated under conditions unfavorable to carbon formation, coke will inevitably be deposited on the active sites of the catalyst. The complicated kinetics that describes the rate of methane conversion using a fluidized Ni/USY-zeolite catalyst able to sustain the oxidation and reduction cycles and suitable to operate under dry reforming conditions is well documented.[9] However, while the types of coke that occur during reforming are thoroughly documented,[10−12] little is known about the modeling of the carbon formation phenomenon, either from a thermodynamic or kinetic standpoint.

The overall goal of the present paper is to explain the formation of coke under dry reforming conditions. The likelihood of coke deposition is evaluated by means of a thermodynamic approach, and is based on the following: (a) the equilibrium constants of the reactions governing the coke formation; (b) a modified noncompetitive Langmuir−Hinshelwood dry reforming rate equation model,[9] and (c) experimental results obtained at CREC−UWO.[8] Also a kinetic model, established on the basis of the thermodynamic analysis, is proposed and tested against experimentally determined coke concentrations.

Coke Formation

Coke formation leads to loss of catalyst activity that occurs via pore blockage, encapsulation of the metal crystals, collapse of the catalyst support, or physical blockage of the tube in fixed bed reformers.[11]

The coke may deposit itself on the nickel catalyst in various forms, all of which have unique characteristics and differences in reactivity. This carbon formation, specifically under conditions of steam reforming, may take place by three routes that result in different kinds of coke.[10] At low temperatures (less than 500 °C), adsorbed hydrocarbons may accumulate on the nickel surface and slowly polymerize into an encapsulating film, blocking and deactivating the nickel surface. At high temperatures (above 600 °C), pyrolitic coke formed by the thermal cracking of hydrocarbons may encapsulate and deactivate the catalyst particle. At tempera-

* To whom correspondence should be addressed. Tel: 1-519-661-2131. Fax: 1-519-661-3498. E-mail: hdelasa@eng.uwo.ca.
[†] University of Western Ontario.
[‡] Universidad Nacional del Sur.
[§] Imperial Oil Research Center.

10.1021/ie0496333 CCC: $30.25
Published on Web 02/04/2005

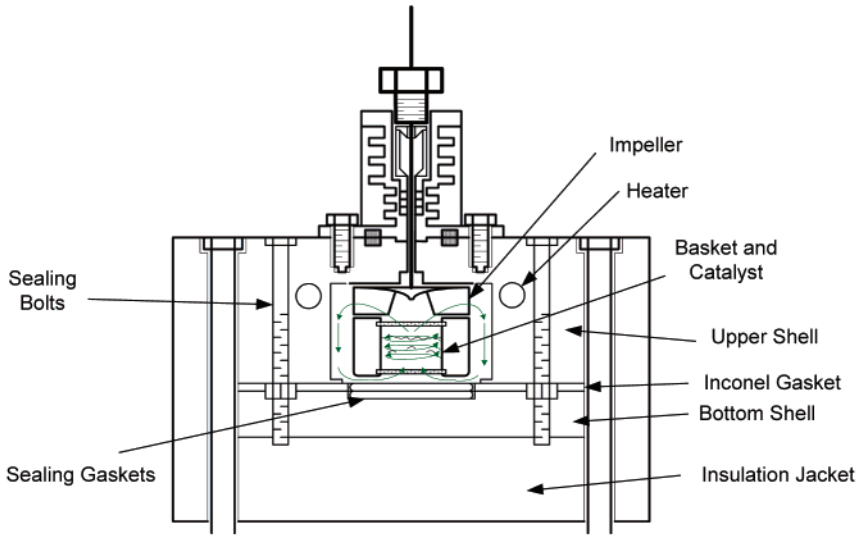

Figure 1. CREC riser simulator. Intense gas recirculation is facilitated by the rotation of an impeller at 3000−6000 rpm.

tures greater than 450 °C, whisker carbon is the principal product of carbon formation via a mechanism involving the diffusion of carbon through nickel crystals, nucleation, and whisker growth with a nickel crystal on the top. The whisker type carbon does not deactivate the nickel surface but rather causes a breakdown of the catalyst by pore plugging.

There are five distinct types of carbon deposits on nickel catalysts from carbon monoxide and hydrocarbons:[13]

(1) C_α: adsorbed atomic carbon (dispersed, surface carbide).

(2) C_β: polymeric films and filaments (amorphous).

(3) C_v: vermicular whiskers/fibers/filaments (polymeric, amorphous).

(4) C_γ: nickel carbide (bulk).

(5) C_c: graphitic platelets and films (crystalline).

It has been reported that under the conditions of dry reforming (700−850 °C), C_v and C_c may be the forms of coke present on the catalyst surface.[8] The C_v or whisker carbons are graphitic and are in general of the same diameter as the metal crystal. Whiskers, tubular in shape, are formed because of the presence of a dissolved carbon concentration gradient in the crystal. The C_c graphitic films diffuse across the Ni particle surface and develop ordered graphite layers parallel to the metal−carbon interface.[8]

Experimental Methods

Under the conditions expected to be used in the Catformer unit, and particularly in the use of methane dry reforming operation, carbon formation may be favored. Although the Catformer concept, using the fluidized Ni/USY-zeolite catalyst,[8,9] is ideal for handling catalyst deactivation due to coke, it is preferable to operate this process in a zone that minimizes carbon formation. As a part of a detailed kinetic study,[9] a set of experiments were designed (following a Taguchi experimental design methodology—which employs a partial factorial design for which all but first- and second-level interactions between factors are removed from the sample space) with the objective of gaining insight into the carbon deposition phenomenon.

Dry reforming experimental runs were conducted in order to characterize the coke selectivity (moles of coke formed per moles of methane converted) on the nickel-based catalyst, over a wide range of industrially relevant conditions. Quantitative independent variables that were augmented over the set of experimental runs were (a) contact time (5−15 s), (b) reaction temperature (700−800 °C), (c) total reactor pressure (5.15×10^5−9.29×10^5 Pa), and (d) feed ratio (CH_4/CO_2 = 1/3−3/1). The catalyst-to-methane ratio was held constant at 34:1 g/g. The catalyst utilized in this research was a fluidizable 20 wt % nickel catalyst supported on ultrastable Y-type zeolite. Catalyst preparation involved several steps including catalyst impregnation, followed by thermal decomposition, calcination, and finally pelletization.[8] Several characterization techniques have previously been employed on this catalyst to measure its performance and stability over time and repeated reduction/oxidation cycles. Results from this characterization study have proven this catalyst to be effective in the Catforming system, under which it is expected that a periodic cycling of the catalyst between reduced (during dry reforming operation) and oxidized (during coke combustion operation) states will occur.[8]

All experimental runs were conducted in the CREC riser simulator reactor.[8,9] This reactor is a bench scale minifluidized bed unit with a capacity of 50 cm^3 and allows the loading of up to 1 g of catalyst. An impeller located in the upper section and a basket containing the catalyst placed in the central section are the main components, as shown in Figure 1. Upon rotation of the impeller at speeds in the range of 3000−6000 rpm, gas is forced outward in the impeller section and downward in the outer reactor annulus. As a result, intense gas mixing occurs providing support for the assumption made in eq 1 of a quasiconstant concentration of reacting species, in effect making this unit ideal for testing fluidizable catalysts.

$$V_R \frac{dC_i}{dt} = \eta r_i w \tag{1}$$

Following the completion of each experiment, the amount of coke was analyzed on the basis of carbon conversion to CO_2. This procedure is called the LECO method, and is one of few standardized methods accepted for this type of analysis. The LECO test is conducted at approximately 1400 °C and in an atmo-

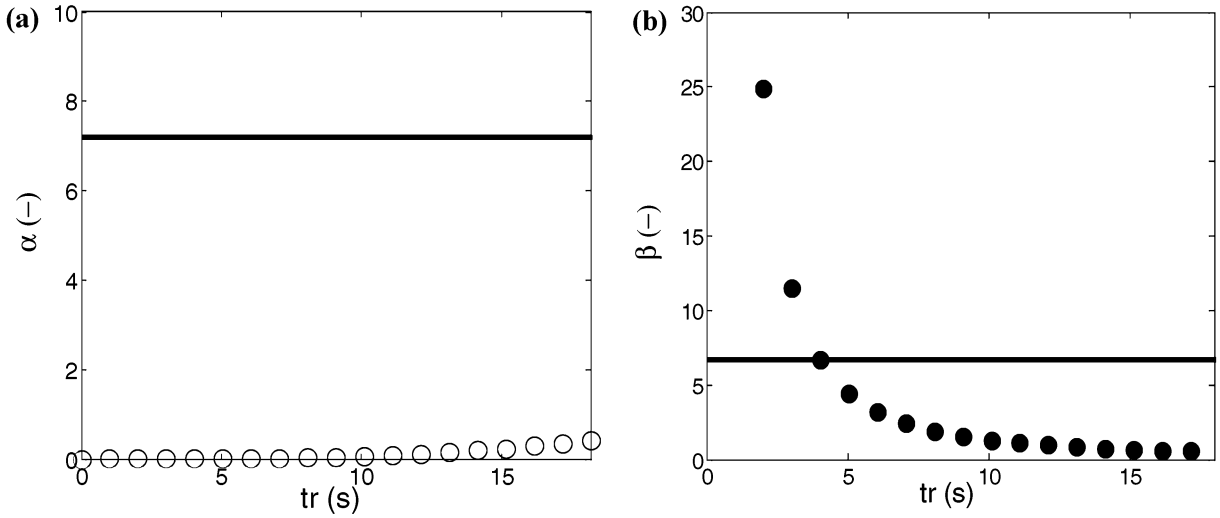

Figure 2. Expected trends for (a) the equilibrium constant K_3 (—) and the parameter α (○) and (b) the equilibrium constant K_4 (—) and the parameter β (●) with the reaction time t_r. $CH_4/CO_2 = 1/3$, $T = 700$ °C, and $P = 9.29 \times 10^5$ Pa.

sphere of excess oxygen, with both of these conditions ensuring that all carbon leaves the system as CO_2. The combustion reaction that occurs, effectively removing coke from the catalyst fully converting the coke into CO_2 is

$$C + O_2 \rightarrow CO_2 \tag{2}$$

Thus, using the stoichiometry of this reaction, the amount of coke can easily be determined from the detection of carbon dioxide by a thermal conductivity detector.

Thermodynamic Analysis of Coke Formation

The mechanism that is generally accepted as the mode of carbon deposition on the catalyst/support structure involves the decomposition of methane and the disproportionation of carbon monoxide:[14−19]

$$CH_4 \rightleftharpoons C + 2H_2 \quad \Delta H^\circ_{298} = 75 \text{ kJ/mol} \tag{3}$$

$$2CO \rightleftharpoons C + CO_2 \quad \Delta H^\circ_{298} = -172 \text{ kJ/mol} \tag{4}$$

As a result of these reactions, different amounts of coke form, depending on the CH_4/CO_2 feed ratio and the operating temperature and pressure. Methane decomposition is an endothermic reaction while carbon monoxide disproportionation is exothermic.

To make possible a quantitative thermodynamic analysis of the above coking reactions, their equilibrium constants were calculated using the following expression:

$$K_i = \exp\left(\frac{-\Delta G_i^\circ}{RT}\right) \tag{5}$$

The Gibbs free energies for reactions 3 and 4 were computed by means of eqs 6 and 7, respectively,[20] which are valid over a wide range of temperatures.

$$\Delta G^\circ = 58886.79 + 270.55T + 0.0311T^2 - (3.00 \times 10^{-6})T^3 + \frac{291405.7}{T} - 54.598T\ln(T) \tag{6}$$

$$\Delta G^\circ = -188030.19 + 402.82T - 0.00524T^2 + \frac{828509.9}{T} - 32.026T\ln(T) \tag{7}$$

In addition, two parameters were defined with respect to the partial pressures of reactants in the dry reforming system ($P_o = 1 \times 10^5$ Pa):

$$\alpha = \frac{p_{H_2}^{\ 2}}{p_{CH_4}}\frac{1}{P_o} \tag{8}$$

$$\beta = \frac{p_{CO_2}}{p_{CO}^{\ 2}}P_o \tag{9}$$

It was postulated that if $K_3 > \alpha$ and $K_4 > \beta$ then coke formation would be thermodynamically favored as this would establish that reactions 3 and 4 had not yet reached thermodynamic equilibrium from the side that promotes coke formation. This indicates that in general, operating conditions for the Catforming process should be sought to minimize the cases where $K_3 > \alpha$ and/or $K_4 > \beta$, and this to minimize coke formation.

Figure 2 presents the trends of both α and β versus their respective equilibrium constants over a 30 s time period for a feed ratio of 1/3, $T = 700$ °C, and $P = 9.29 \times 10^5$ Pa. The parameters α and β were calculated from the partial pressures of H_2, CH_4, CO, and CO_2 determined by means of the following rate equation under the corresponding experimental conditions:[8]

$$r_{CH_4} = \frac{-kK_{CO_2}K_{CH_4}\left(p_{CH_4}p_{CO_2} - \dfrac{p_{H_2}^{\ 2}p_{CO}^{\ 2}}{K_{DR}}\right)}{1 + K_{CH_4}p_{CH_4} + K_{CO_2}p_{CO_2}} \tag{10}$$

Table 1 reports the preexponential coefficients k_o, $K^o_{CH_4}$, and $K^o_{CO_2}$ and the activation energies E, E_{CH_4}, and E_{CO_2} for the 20 wt % Ni/USY-zeolite catalyst.

The partial pressures of each of the chemical species were assessed using the modified noncompetitive Langmuir−Hinshelwood model (eq 10), and the extents of the dry reforming and the water−gas shift reactions (eqs 11 and 12, respectively) for the measured experimental

Table 1. Preexponential and Activation Energy Values Evaluated Using a 20 wt % Ni/USY Catalyst with Linearized 95% Confidence Interval for Modified Noncompetitive Langmuir−Hinshelwood Model

	$k_o \times 10^{6\,a}$	$E \times 10^{-6}$	$K^o_{CH_4} \times 10^{3\,b}$	$E_{CH_4} \times 10^{-6}$	$K^o_{CO_2} \times 10^{3\,c}$	$E_{CO_2} \times 10^{-6}$
units	mol g_{cat}^{-1} s^{-1}	J mol^{-1}	Pa^{-1}	J mol^{-1}	Pa^{-1}	J mol^{-1}
estimate	1.45	1.04	−4.50	1.01	−3.61	1.12
interval	0.81	0.088	2.22	0.087	1.34	0.098

[a] $k = k_o \exp[(-E/R)[(1/T) - (1/T_c)]]$. [b] $K_{CH_4} = K^o_{CH_4} \exp[(E_{CH_4}/R)[(1/T) - (1/T_c)]]$. [c] $K_{CO_2} = K^o_{CO_2} \exp[(E_{CO_2}/R)[(1/T) - (1/T_c)]]$.

conditions. The noncompetitive Langmuir−Hinshelwood rate model, eq 10, considers the adsorption of CH_4 and CO_2 to occur on different sites of the catalyst, with the CH_4 adsorption site possibly being the zeolite support, and the CO_2 adsorption site possibly being the nickel crystal.[8,9] This model does not consider the effects of carbon deposition on these active catalyst sites. Furthermore, compared to other mechanistic rate expressions for the dry reforming of CH_4, it must be mentioned that the modified noncompetitive Langmuir−Hinshelwood model has been statistically shown to be the most accurate model for explaining the mechanism by which the dry reforming of CH_4 proceeds.[8,9]

$$CH_4 + CO_2 \rightleftharpoons 2CO + 2H_2 \tag{11}$$

$$CO + H_2O \rightleftharpoons CO_2 + H_2 \tag{12}$$

Because the bench-scale fluidized riser simulator operates as an isothermal well-mixed batch reactor, the extent of the dry reforming reaction, ϵ_{DR}, was calculated by integration of the methane mass balance.[8,9]

$$\frac{d\epsilon_{DR}}{dt} = -r_{CH_4} w \tag{13}$$

As the water−gas shift reaction was found to be very close to chemical equilibrium,[8,9] the extent of reaction 12, ϵ_{WGS}, was estimated using the chemical equilibrium relationship

$$K_{WGS} = \frac{p_{CO_2} p_{H_2}}{p_{CO} p_{H_2O}} \tag{14}$$

Based on the initial number of moles of methane and carbon dioxide injected, the partial pressures of the species present were computed as

$$p_{CH_4} = P\left(\frac{N^o_{CH_4} - \epsilon_{DR}}{N^o_T}\right) \tag{15}$$

$$p_{CO_2} = P\left(\frac{N^o_{CO_2} - \epsilon_{DR} - \epsilon_{WGS}}{N^o_T}\right) \tag{16}$$

$$p_{CO} = P\left(\frac{N^o_{CO} + 2\epsilon_{DR} + \epsilon_{WGS}}{N^o_T}\right) \tag{17}$$

$$p_{H_2} = P\left(\frac{N^o_{H_2} + 2\epsilon_{DR} - \epsilon_{WGS}}{N^o_T}\right) \tag{18}$$

$$p_{H_2O} = P\left(\frac{N^o_{H_2O} + \epsilon_{WGS}}{N^o_T}\right) \tag{19}$$

$$P = \frac{N_T R T}{V_R} \tag{20}$$

Equations 16−19 were substituted back into eq 14 and the extent, ϵ_{WGS}, was calculated from the following quadratic relationship:

$$\epsilon_{WGS} = \frac{-b - \sqrt{b^2 - 4ac}}{2a} \tag{21}$$

with

$$a = 1 - K_{WGS} \tag{22}$$

$$b = -(\epsilon_{DR} + 2K_{WGS}\epsilon_{DR} + N^o_{CO_2}) \tag{23}$$

$$c = 2\epsilon_{DR}(N^o_{CO_2} - \epsilon_{DR}) \tag{24}$$

Figure 2a indicates that $K_3 > \alpha$ for all reaction times (t_r). In fact, this was the result for all conditions tested. Hence, it can be stated that reaction 3 may always develop in the direction favoring coke formation. Figure 2b shows that initially $\beta > K_4$, and thus, until the time t_c, when β crosses K_4, reaction 4 is in a region of decoking.

Following from the observed trends for the α and β parameters, it can be approximated that during the time when $\beta > K_4$ no coke formation occurs, as there is a balance of coke formation via reaction 3, and decoking via reaction 4. Considering this approximation, the time t_c when β crosses K_4 was determined for all experimental conditions. Figure 3 reports a plot of t_c versus temperature and pressure for all feed ratios. It can be seen that t_c increases substantially from augmenting the temperature from 700 °C to 800 °C, with this trend being established for all feed ratios. Also, Figure 3 elucidates the significant relationship between t_c and the feed ratio. For a lower feed ratio, the time that the Boudouard reaction remains in the decoking region is greater. This effect of feed ratio on t_c seems to be less significant at higher feed ratios. Furthermore, Figure 3 illustrates the relationship between pressure and t_c, with t_c slightly

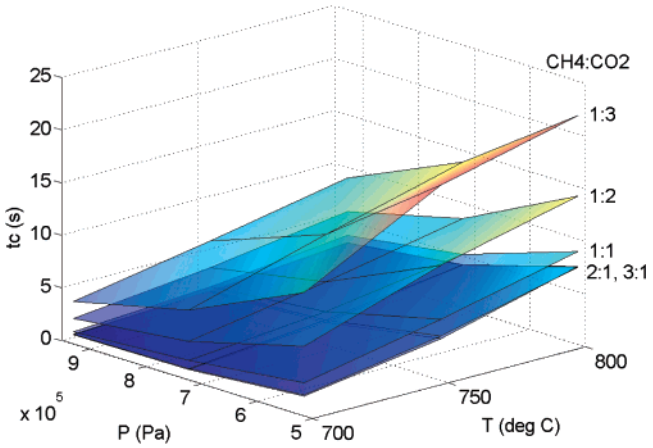

Figure 3. Time t_c (when β crosses K_4) versus temperature and pressure for all feed ratios.

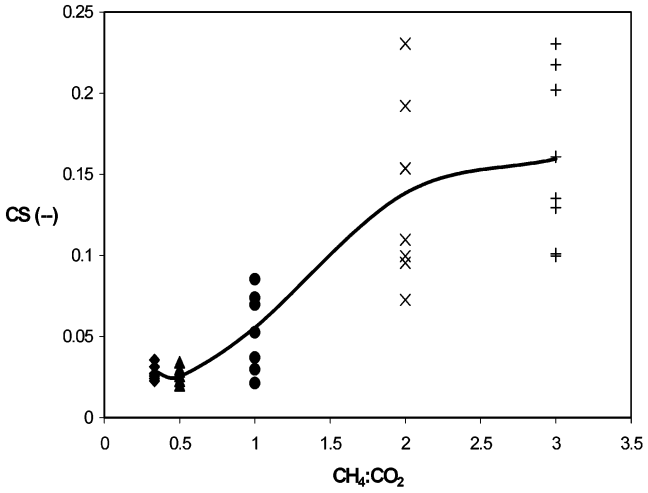

Figure 4. Coke selectivity as a function of CH_4/CO_2 feed ratio. CH_4/CO_2 = 1:3 (◆), = 1:2 (▲), = 1:1 (●), = 2:1 (×), = 3:1 (+). Average CS trend line (—).

decreasing with increasing pressure, a trend that is thermodynamically expected for the carbon monoxide disproportionation reaction 4. This effect apparently becomes more significant as the temperature is increased from 700 to 800 °C and the feed ratio is decreased from 3:1 to 1:3.

With respect to coke selectivity (CS = moles of coke formed/moles of methane converted), the significance of the observed trends for t_c is verified by comparing these trends with those found for the coke selectivity versus feed ratio. It has been reported that coke selectivity rises with increasing feed ratio. As shown in Figure 4,[8] there is a region of low coking below $CH_4/CO_2 = 1$, and the coke selectivity rises with increasing feed ratio, until a region of high coking is reached at $CH_4/CO_2 = 2$.

Comparing the trends of the time, t_c, when the carbon monoxide disproportionation reaction begins to favor coke formation, and coke selectivity, CS, (Figures 3 and 4, respectively) from a qualitative viewpoint, while holding pressure and temperature constant and manipulating feed ratio, it can be stated that as t_c tends to decrease with increasing feed ratio the coke selectivity rises quite dramatically.

Figure 5 shows an example of this trend with the reactor conditions set at a temperature of 750 °C and 7.22×10^5 Pa pressure. Under these conditions, while CH_4/CO_2 increases from 1/3 to 3, t_c decreases from 10.64 s to 2.05 s, and CS increases from 0.02 to 0.16 molC/molCH_4. This evidence suggests that the time when β crosses the equilibrium line (shown in Figure 3) plays a significant role in the extent of coke formation; and this would be expected if the carbon monoxide disproportionation reaction 4 is the dominant route of coke formation. The fact the coke selectivity increases with decreasing t_c (time required to achieve $K_4 > \beta$) justifies this, in that for a greater t_c there is less time spent by the dry reforming system in the coking region, and conversely for a smaller t_c there is more time spent by the system in the coking region, and thus a higher *CS* value results. Furthermore, the effect of temperature on t_c (Figure 3) implies that the extent of carbon deposition (i.e. *CS*) during dry reforming decreases at higher reaction temperature, indicating that the exothermic carbon monoxide disproportionation constitutes the main contribution to coke formation.

The above analysis yielded an important thermodynamic result of the dry reforming system under study

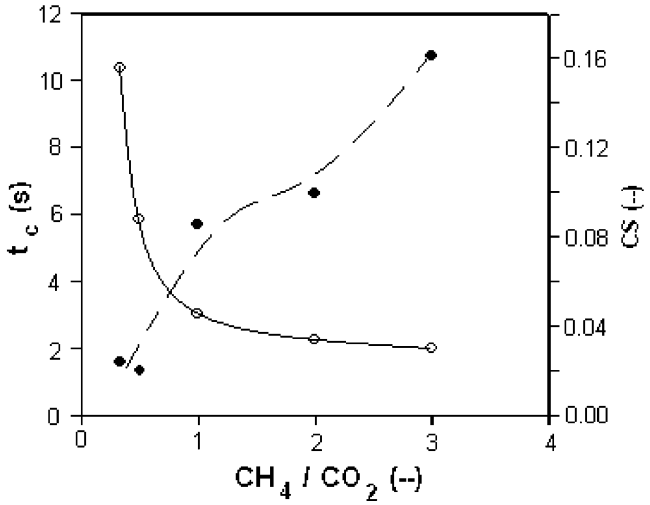

Figure 5. Coke selectivity (CS, ●; trend line, - - -) and time when carbon monoxide disproportionation reaction enters region of coke formation (t_c, ○; trend line, —) plotted against feed ratio at T = 750 °C and $P = 7.22 \times 10^5$ Pa.

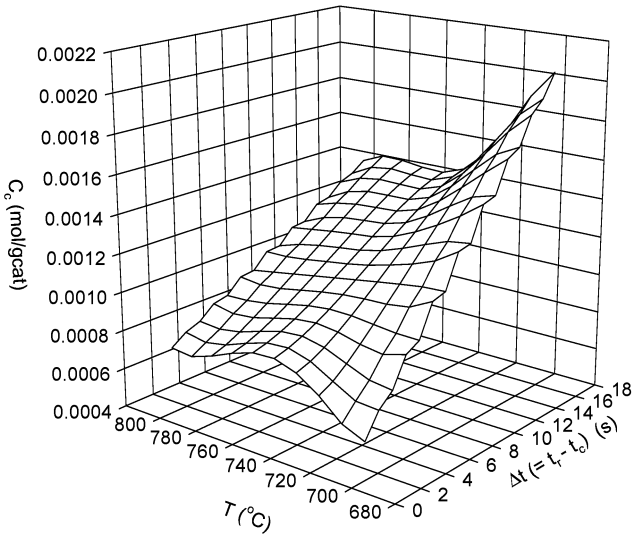

Figure 6. Coke concentration (C_c) versus Δt and temperature for $CH_4/CO_2 = 1$.

that is in agreement with data reported in the literature.[21,22] Based on this result and the existence of a strong relationship between t_c and *CS*, kinetic modeling of the coke formation mechanism was established.

Kinetic Modeling

The approach taken to kinetically model the deposition of coke on the active sites (most probably the nickel crystals[8,9]) of the catalyst utilized the thermodynamic analysis described above, and in this, two important assumptions were made:

(a) No net coke formation occurs during the period when α is in the coking region and β is in the decoking region ($C_c|_{t=t_c} = 0$).

(b) Coke begins to accumulate only after the carbon monoxide disproportionation reaction begins to thermodynamically favor this carbon deposition; and this coke formation occurs at a rate, r_c.

Following from these assumptions, it was desired to determine the trend in the coke selectivity over a range of reaction times and temperatures. Figure 6 shows a plot of the coke concentration ($C_c \equiv$ mol C/gcat) versus Δt ($= t_r - t_c$) and temperature, with $CH_4/CO_2 = 1$ and

Table 2. Regression Analysis for Most Significant Rate Expressions Describing Coke Formation in the CREC Riser Simulator

model		I	II	III
r		$k_{app}p_{CO}$	k_{app}	$k_{app}\dfrac{\left(p_{CO}^{\,2}-\dfrac{p_{CO_2}}{K_{eq}}\right)}{p_{CO}^{\,3}}$
σ^a		0.693	0.389	0.256
$k_{app,o}{}^b$		5.36×10^{-10} mol/Pa g_{cat} s	1.49×10^{-4} mol/g_{cat} s	3.06×10^{1} mol Pa/g_{cat} s
lb[c]	ub		1.23×10^{-4} 1.75×10^{-4}	2.68×10^{1} 3.44×10^{1}
E_{app}		2.00×10^{4} J/mol	1.35×10^{4} J/mol	2.60×10^{4} J/mol
lb[c]	ub		-2.32×10^{-4} 5.01×10^{-4}	8.81×10^{1} 5.19×10^{4}

[a] $\sigma = \sqrt{\sum((C_{c,mod}-C_{c,exp})/C_{c,avg})^2/(n-1)}$; where $C_{c,avg} = (C_{c,mod} + C_{c,exp})/2$. [b] $k_{app} = k_{app,o} \exp[(-E_{app}/R)\,[(1/T) - (1/T_c)]]$; where the centered value T_c is the average temperature for all experimental runs. [c] The lower and upper bounds (lb and ub) are calculated at 95% confidence level. For model II, lb and ub on k_{app} and E_{app} could not be found as the Matlab regression program gave erroneous values for these limits.

all pressures. It can be seen that the concentration of coke decreases with increasing temperature; while this concentration rises by increasing the amount of time spent by the carbon monoxide disproportionation reaction 4 in the coke formation regime. This trend was also observed for feed ratios both below and above $CH_4/CO_2 = 1$.

Regarding the observed trends between C_c and Δt, various kinetic models were postulated to predict the coke selectivity over a range of temperatures, pressures, and contact times.

Table 2 lists the most significant kinetic models describing the rate of coke formation that were tested. Model I represents a first order rate equation considering only the carbon monoxide contribution. Model II describes zero order kinetics, and model III results from taking into account the carbon monoxide disproportionation, the reverse of this reaction and a CO adsorption step at equilibrium. Under the studied dry reforming conditions model III constitutes the best fit.

The results of the regression analysis (Table 2) indicate that by decreasing the overall order of the rate expression from +1 to −1, a better fit to the experimentally determined coke is obtained. Model I, with an overall order of 1, proves to be very weak in predicting coke formation, with $\sigma = 0.693$. Decreasing the order of the reaction to zero (model II) dramatically improves the accuracy of the model, with $\sigma = 0.389$. However, the lower bound on the estimated activation energy (E_{app}) for this model renders the prediction statistically insignificant at the 95% confidence level. Further decreasing of the overall order of the rate expression to −1 (model III) shows a very significant increase in predictive accuracy, with $\sigma = 0.256$. This model also gives much more reasonable lower and upper bounds on both estimated parameters. The estimated preexponential factor is $k_{app,o} = 30.6 \pm 3.8$ mol Pa/g_{cat} s, and the estimated apparent activation energy of the lumped rate constant is $E_{app} = 2.60 \times 10^4$ J/mol, with a lower bound, lb = 8.81×10^1 J/mol, and upper bound, ub = 5.19×10^4 J/mol.

Figure 7 shows a plot of the reconciliation between the experimentally observed coke concentration and those predicted using the parameter estimates for model III. Upon inspection of these results, it can be seen that almost all predictions made by model III are within the calculated σ value at every level of coke formation.

Regarding the adsorption of hydrogen, no significant effect on the rate of coke formation was noticed from the regression analysis. This is not surprising given that the above-described thermodynamic study suggested

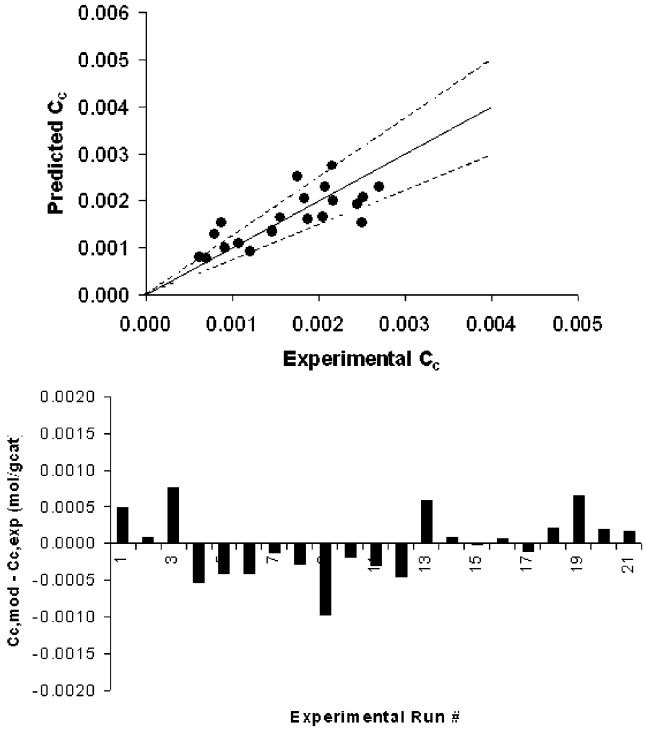

Figure 7. Reconciliation plot showing the results when parameters are estimated using model III for predicting coke formation in the CREC riser simulator (- - - $\pm\sigma$).

that carbon monoxide disproportionation is the dominant coke-forming reaction.

According to the best-obtained rate expression (model III), the reaction mechanism requires three adjacent free catalyst sites. In fact, this kinetic model constitutes a simplification of the rate equation derived from supposing that the following reaction sequence takes place.

For the initial reaction step

$$CO + S_1 \rightleftharpoons COS_1 \quad (25)$$

$$CO + S_2 \rightleftharpoons COS_2 \quad (26)$$

$$COS_1 + COS_2 \rightleftharpoons CO_2S_1 + CS_2 \quad (27)$$

$$CO_2S_1 \rightleftharpoons CO_2 + S_1 \quad (28)$$

$$CS_2 \rightleftharpoons C + S_2 \quad (29)$$

with COS_1 and COS_2 representing the CO adsorbed on sites of type S_1 and S_2, and CO_2S_1 and CS_2 representing the adsorbed CO_2 and coke on S_1 and S_2 sites, respectively.

For the following reaction step to proceed, given the site S_2 is now occupied by coke, the reaction has to involve another adjacent site, S_3,

$$CO + S_1 \rightleftharpoons COS_1 \tag{30}$$

$$CO + S_3 \rightleftharpoons COS_3 \tag{31}$$

$$COS_1 + COS_3 \rightleftharpoons CO_2S_1 + CS_3 \tag{32}$$

$$CO_2S_1 \rightleftharpoons CO_2 + S_1 \tag{33}$$

$$CS_3 \rightleftharpoons C + S_3 \tag{34}$$

with COS_1 and COS_3 representing the CO adsorbed on sites of type S_1 and S_3, and CO_2S_1 and CS_3 representing the adsorbed CO_2 and coke on S_1 and S_3 sites, respectively.

Thus, considering the forward reaction, it can be seen from the suggested reaction sequence that the rate of coke formation is a function not only of the availability of two sites for CO adsorption (S_1 and S_2) but also of the availability of an extra free site (i.e., S_3) adjacent to the CO adsorbed, with each cycle consuming one adjacent free site: if there is no adjacent free site then the reaction cannot proceed in the forward direction. Consequently, the rate expression for the forward coke forming reaction should be described by

$$\vec{r}_c = \vec{k}\theta_{CO}\theta_{CO}\theta_v \tag{35}$$

Assuming all CO adsorption steps to be at quasithermodynamic equilibrium, the above equation becomes

$$\vec{r}_c = \vec{k}K_{CO}{}^2p_{CO}{}^2\theta_v{}^3 \tag{36}$$

Taking into account the reverse reaction only, the rate expression is a function of the availability of "CS_i" sites adjacent to the sites occupied by CO_2 and C. Each cycle consumes a "CS_i" site. Consequently, the rate equation for this reverse reaction is represented by

$$\overleftarrow{r}_c = \overleftarrow{k}\theta_{CO_2}\theta_C\theta_C \tag{37}$$

Upon substitution of the adsorption equilibrium expressions and assuming $a_c = 1$, the previous equation turns into

$$\overleftarrow{r}_c = \overleftarrow{k}K_{CO_2}K_C{}^2p_{CO_2}\theta_v{}^3 \tag{38}$$

Finally, considering both the forward and reverse reactions, and adopting the Langmuir isotherm to determine θ_v, the overall rate equation becomes

$$r_c = \frac{\vec{k}K_{CO}{}^2p_{CO}{}^2 - \overleftarrow{k}K_{CO_2}K_C{}^2p_{CO_2}}{(1 + K_C + K_{CO}p_{CO} + K_{CO_2}p_{CO_2})^3} \tag{39}$$

From the regression analysis, it was found that $K_{CO}p_{CO} \gg 1 + K_C + K_{CO_2}p_{CO_2}$. This allows simplifying eq 39, so that a single lumped parameter (k_{app}) can be used in the regression

$$r = k_{app}\frac{\left(p_{CO}{}^2 - \dfrac{p_{CO_2}}{K_{eq}}\right)}{p_{CO}{}^3} \tag{40}$$

In this expression, $k_{app} = \vec{k}/KCO$, where $\vec{k}$ is the forward rate constant of reaction 27 and K_{CO} is the adsorption constant for carbon monoxide. K_{eq} represents the equilibrium constant of the CO disproportionation reaction 4.

As the amount of coke formation is quite low in comparison to the total number of available catalyst sites, the following two simplifications in eq 39 are adequate under the experimental conditions of this study, (a) $K_C \ll 1$ and, (b) there is no catalyst decay parameter required in the kinetic model. The fact given that the catalyst does not exhibit any significant deactivation can be attributed to the formation of filamentous whisker carbon. This whisker-type carbon, which keeps intact the nickel particles that are lifted from the support during their growth, does not deactivate the catalyst as long as no excess coke is accumulated.[10,17] Only their accumulation finally plugging the pores of the catalyst or completely encapsulating the nickel particles in filament nodes results in deactivation. It has been reported that the rate-determining step for the formation of filamentous whisker carbon is the diffusion of carbon through a metal particle.[23] The driving force for this diffusion process is considered to be heat generated by exothermic surface processes, such as CO adsorption and disproportionation.[16]

The modified noncompetitive Langmuir−Hinshelwood dry reforming rate equation for the 20 wt % Ni/USY-zeolite catalyst and the experimental conditions under study,[8,9] incorporates a $K_{CO_2}p_{CO_2}$ which indicates a strong adsorption of CO_2 on the nickel surface. One should argue that consistent with this, carbon dioxide adsorption should be kept in the denominator of the rate expressions for the coke formation. However, in practice and in agreement with previous kinetic studies of coke formation,[24,25] the effect of CO_2 in eq 39 is shown to be negligible. This result can be attributed to the fact that after coke is deposited the carbon covering the surface leads to an enhanced CO adsorption in the near carbon sites.[26] Given that eq 39 describes the rate of coke formation only after t_c (when a net coke formation begins, as suggested by assumption (1)) and that CO adsorption increases considerably in the near-coke regions, the considerations leading eq 39 into eq 40 are valid.

In summary, it was found that the proposed kinetic model under the thermodynamic constraints of coke formation, $K_4 > \beta$, is a sound rate expression consistent with expected mechanistic reaction rate formulation.

Conclusions

The results of this study of coke formation on a 20 wt % Ni/USY-zeolite catalyst for the dry reforming process can be summarized as follows:

(1) Thermodynamic analysis elucidated the significance of the carbon monoxide disproportionation reaction on the amount of coke formed over a 20 wt % Ni/USY-zeolite catalyst. By defining thermodynamic parameters (α and β) quantification of the effects of this reverse Boudouard reaction is possible.

(2) A correlation was found between coke selectivity (CS) and the time the carbon monoxide disproportionation reaction favors coke formation (t_c).

(3) Kinetic analysis quantified the relationship between coke formation and the amount of time spent by this dry reforming system under conditions promoting coke deposition, as predicted by the thermodynamic study.

(4) A negative overall order model of one with respect to the partial pressure of carbon monoxide was found as the most accurate prediction of the rate of coke formation. This type of kinetics strongly suggests the requirement of three adjacent free catalyst sites for the coking reaction to proceed under allowable thermodynamic constraints.

Nomenclature

a = quadratic equation parameter, eq 22
a_c = carbon activity
b = quadratic equation parameter, eq 23
$C_{c,i}$ = coke concentration; i = mod, exp, avg (mol C/g_{cat})
C_i = concentration of species i (mol i/m^3)
CS = coke selectivity (mol C/mol CH_4)
c = quadratic equation parameter, eq 24
E = activation energy for methane conversion (J/mol)
E_{app} = apparent activation energy for coke formation (J/mol)
E_i = heat of adsorption for component i; i = CH_4, CO_2 (J/mol)
ΔG_i° = standard Gibbs free energy for reaction i; i = 3, 4
ΔH_{298}° = standard heat of reaction (J/mol)
K_3 = equilibrium constant for the CH_4 decomposition reaction
K_4 = equilibrium constant for the CO disproportionation reaction
K_{eq} = equilibrium constant for the CO disproportionation reaction in terms of partial pressures; $K_{eq} = K_4/P_o$ (Pa^{-1})
K_C = adsorption constant for coke
K_{CH_4} = adsorption constant for methane (Pa^{-1})
$K_{CH_4}^o$ = preexponential factor, adsorption constant for methane (Pa^{-1})
K_{CO} = adsorption constant for carbon monoxide (Pa^{-1})
K_{CO_2} = adsorption constant for carbon dioxide (Pa^{-1})
$K_{CO_2}^o$ = preexponential factor, adsorption constant for carbon dioxide (Pa^{-1})
K_{DR} = equilibrium constant the dry reforming reaction
K_{WGS} = equilibrium constant for the water−gas shift reaction
k = rate constant for methane conversion (mol/g_{cat}·s)
k_o = preexponential factor, rate constant for methane conversion (mol/g_{cat}·s)
$\vec{k}$ = forward rate constant for reaction 27 (mol C/g_{cat}·s·Pa^2)
$\overleftarrow{k}$ = reverse rate constant for reaction 27 (mol C/g_{cat}·s·Pa).
k_{app} = rate constant for coke formation (mol C/g_{cat}·Pa^d; d: dependent on kinetic model)
$k_{app,o}$ = preexponential factor (mol C/g_{cat} Pa^d; d: dependent on kinetic model)
n = number of experiments
N_i^o = initial moles of species i; i = H_2, CO, CO_2, CH_4, H_2O (mol)
N_T^o = total number of initial moles (mol)
P_o = reference pressure (Pa)
P = total reactor pressure (Pa)
p_i = partial pressure of component i; i = H_2, CO, CO_2, CH_4, H_2O (Pa)
r_c = rate of coke formation (mol C/g_{cat}·s)
r_{CH_4} = rate of conversion of methane (mol CH_4/g_{cat}·s)
r_i = rate of conversion of species i (mol i/g_{cat}·s)
R = universal gas constant (J/mol·K)
S_i = vacant catalyst site i; i = 1−3
T = temperature (K)
T_c = average temperature of all experimental conditions (K)
t = reaction time (s)
t_c = time required for $K_4 > \beta$ to become satisfied (s)
t_r = total reaction time (s)
V_R = reactor volume (m^3)
w = catalyst weight (g_{cat})

Subscripts

avg = average value
exp = experimental value
mod = value predicted by model III

Greek Symbols

α = thermodynamic parameter related to CH_4 decomposition reaction
β = thermodynamic parameter related to CO disproportionation reaction
$\Delta t = t_r - t_c$ (s).
ϵ_i = extent of reaction i; i = DR, WGS (mol i)
η_i = effectiveness factor
θ_i = fraction of catalyst sites occupied by species i; i = C, CO, CO_2
σ = standard deviation

Literature Cited

(1) Mark, M. F.; Maier, W. F. CO_2−Reforming of Methane on Supported Rh and Ir Catalysts. *J. Catal.* **1996**, *164*, 122.

(2) Zhang, Z. L.; Verykios, X. E. Carbon dioxide reforming of methane to ssynthesis gas over supported Ni catalysts. *Catal. Today* **1994**, *21*, 589.

(3) Blom, R.; Dahl, I. M.; Slagtern, A.; Sortland, B.; Spjelkavik, A.; Tangstad, E. Carbon Dioxide Reforming of Methane over Lanthanum-modified Catalysts in a Fluidized-bed reactor. *Catal. Today* **1994**, *21*, 535.

(4) Tsipouriari, V. A.; Efstathiou, A. M.; Zhang, Z. L.; Verykios, X. E. Reforming of Methane with Carbon Dioxide to Synthesis Gas over Supported Rh Catalysts. *Catal. Today* **1994**, *21*, 579.

(5) Gadalla, A. M.; Bower, B. The Role of Catalyst Support on the Activity of Nickel for Reforming Methane with CO_2. *Chem. Eng. Sci.* **1988**, *43* (11), 3049.

(6) Teuner, St. C.; Neumann, P.; Von Linde, F. The Calcor Standard and Calcor Economy Processes. *Oil Gas Eur. Mag.* **2001**, *3*, 44.

(7) Udengaard, N. R.; Bak Hansen, J. H.; Hanson, D. C.; Stal, J. A. Sulfur promoted Reforming Process lowers Syngas Hydrogen/Carbon Monoxide Ratio. *Oil Gas J.* **1992**, *90* (10), 62.

(8) El Solh, T. Dry Reforming of Methane in a Fast Fluidized Bed Reactor Catalysis and Kinetics. Ph.D. Thesis, University of Western Ontario, London, Ontario, 2002.

(9) El Solh, T.; Jarosch, K.; de Lasa, H. Catalytic Dry Reforming of Methane in a CREC Riser Simulator Kinetic Modeling and Model Discrimination. *Ind. Eng. Chem. Res.* **2003**, *42*, 2507.

(10) Rostrup-Nielsen, J. R. *Catalytic Steam Reforming. Catalysis—Science and Technology*; Anderson, J. R., Boudart, M., Eds.; Springer-Verlag: Berlin, Heidelberg, 1984; Vol. 5, p 1.

(11) Rostrup-Nielsen, J. R. Industrial Relevance of Coking. *Catal. Today* **1997**, 37.

(12) Lee, S. *Methane and its Derivatives*; Marcel Dekker: New York, NY, 1997.

(13) Bartholomew, C. H. Mechanism of Catalyst Deactivation. *Applied Catal. A: General* **2001**, *212*, 17.

(14) Rostrup-Nielsen, J. R.; Bak Hansen, J.-H. CO_2−Reforming of Methane over Transition Metals. *J. Catal.* **1993**, *144*, 38.

(15) Wang, S.; Lu, G. Q. Carbon Dioxide Reforming of Methane To Produce Synthesis Gas over Metal-Supported Catalysts: State of the Art. *Energy Fuels* **1996**, *10*, 896.

(16) Bradford, M. C. J.; Vannice, M. A. Catalytic Reforming of Methane with Carbon Dioxide over Nickel Catalysts I. Catalyst deactivation and activity. *Appl. Catal. A: Gen.* **1996**, *142*, 73.

(17) Pinaeva, L.; Schuurman, Y.; Mirodatos, C. *Carbon Routes in Carbon Dioxide Reforming of Methane. Environmental Challenges and Greenhouse Gas Control for Fossil Fuel Utilization in the 21st Century*; Kluwer Academic/Plenum Publishers: New York, 2002.

(18) Olsbye, U.; Moen, O.; Slagtern, A.; Dahl, J. M. An Investigation of the Coking Properties of Fixed and Fluid Bed Reactors during Methane-to-Synthesis Gas Reactions. *Appl. Catal. A: Gen.* **2002**, *228*, 289.

(19) Liu, B. S.; Au, C. T. Carbon Deposition and Catalyst Stability over La_2NiO_4/γ-Al_2O_3 during CO_2 Reforming of Methane to Syngas. *Appl. Catal. A: Gen.* **2003**, *244*, 18.

(20) Smith, J. M.; Van Ness, H. C.; Abbott, M. M. *Introduction to Chemical Engineering Thermodynamics*; The McGraw-Hill Companies, Inc.; New York, 1996.

(21) Bradford, M. C. J.; Vannice, M. A. CO_2 Reforming of CH_4. *Catal.Rev. Sci. Eng.* **1999**, *41* (1), 1.

(22) Swaan, H. M.; Kroll, V. C. H.; Martin, G. A.; Mirodatos, C. Deactivation of Supported Nickel Catalysts during the Reforming of Methane by Carbon Dioxide. *Catal. Today* **1994**, *21*, 571.

(23) Rodriguez, N. M. A Review of Catalytically Grown Carbon Nanofibers. *J. Mater. Res.* **1993**, *38* (4), 858.

(24) Tavares, N. T.; Alstrup, J.; Bernando, C. A.; Rostrup-Neilsen, J. R. CO Disproportionation on Silica-supported Nickel and Nickel−Copper Catalysts. *J. Catal.* **1994**, *147*, 525.

(25) Snoeck, J.-W.; Froment, G. F.; Fowles, M. Steam/CO_2 Reforming of Methane. Carbon Filament Formation by the Boudouard Reaction and Gasification by CO_2, by H_2, and by Steam: Kinetic Study. *Ind. Eng. Chem. Res.* **2002**, *41*, 4252.

(26) Vink, T. J.; Van Zandvoort, M. M. J.; Gijzeman, O. L. J.; Geus, J. W. The Interaction of Oxygen and Carbon Monoxide with a Carbided Ni(111) Surface. *Appl. Surface Sci.* **1984**, *18*, 255.

Received for review May 4, 2004
Revised manuscript received October 8, 2004
Accepted October 18, 2004

IE0496333